Modeling of Interphases in Fiber-Reinforced Composites Under Transverse Loading Using the Boundary Element Method

Y. J. Liu[1]
Assistant Professor,
e-mail: Yijun.Liu@uc.edu
Mem. ASME

N. Xu
Graduate Student
Department of Mechanical, Industrial,
and Nuclear Engineering,
P.O. Box 210072,
University of Cincinnati,
Cincinnati, OH 45221-0072

J. F. Luo
Graduate Student,
Department of Mechanical Engineering,
University of California,
Berkeley, CA 94720-1740

In this paper, interphases in unidirectional fiber-reinforced composites under transverse loading are modeled by an advanced boundary element method based on the elasticity theory. The interphases are regarded as elastic layers between the fiber and matrix, as opposed to the spring-like models in the boundary element method literature. Both cylinder and square unit cell models of the fiber-interphase-matrix systems are considered. The effects of varying the modulus and thickness (including nonuniform thickness) of the interphases with different fiber volume fractions are investigated. Numerical results demonstrate that the developed boundary element method is very accurate and efficient in determining interface stresses and effective elastic moduli of fiber-reinforced composites with the presence of interphases of arbitrarily small thickness. Results also show that the interphase properties have significant effect on the micromechanical behaviors of the fiber-reinforced composites when the fiber volume fractions are large.
[S0021-8936(00)02501-0]

1 Introduction

Interphases, or interfacial zones, in fiber-reinforced composite materials are the thin layers between the fiber and matrix (Fig. 1). These interphases are formed due to, for example, chemical reactions between the fiber and matrix materials, or the use of protective coatings on the fiber during manufacturing. The fiber, which is employed to reinforce the matrix material in the fiber direction, is usually much stiffer than the matrix material. Different levels of stresses and deformations can develop in the fiber and matrix materials, because of this mismatch in the material properties. It is the interphases that bond the fiber and matrix together to ensure the desired functionality of the composite material under external loads. Although small in thickness, interphases can significantly affect the overall mechanical properties of the fiber-reinforced composites, as observed in many studies ([1–9]). It is the weakest link in the load path, and consequently most failures in fiber-reinforced composites, such as debonding, fiber pullout, and matrix cracking, occur in or near this region. Thus, it is crucial to fully understand the mechanism and effects of the interphases in fiber-reinforced composites. Numerical techniques such as the finite element method and the boundary element method are indispensable tools in serving this purpose.

Numerical modeling of fiber-reinforced composite materials presents great challenges to both the finite element method and boundary element method especially for the analysis at the microstructural level. The main issue in the micromechanics analysis of fiber-reinforced composites is to predict the interface stresses for durability assessment, and to determine the engineering properties, such as the effective Young's moduli, Poisson's ratios, and thermal expansion coefficients needed for structural analysis. Idealized models using the unit cell (or representative volume element) concept are usually employed in micromechanics analysis, in which the fibers are assumed to be infinitely long and packed in a square or hexagonal pattern (see, e.g., [10,11,12]). Although only one fiber and the surrounding matrix are modeled in the unit cell approach, the presence of the interphase between the fiber and matrix still makes the finite element method and boundary element method modeling difficult, simply because of the thinness of the interphases which are at the micrometer level or below.

Many finite element models based on the two-dimensional elasticity theory have been developed to study the micromechanical properties of fiber-reinforced composites under transverse loading and with the presence of an interphase, for example, in [13,6,14], and [8], and most recently in [9]. In all these finite element method models, a layer of very fine finite elements was used between the fiber and matrix to model the interphase. Because of the thinness of the interphase, a large number of small finite elements are needed in these models, in order to avoid elements with large aspect ratios which can deteriorate the finite element method solutions. This, in turn, causes a large number of elements in the fiber and matrix regions because of the connectivity requirement in the finite element method. For instance, in [9], more than 3500 finite elements were used to model only *one quarter* of the chosen unit cell. With further smaller thickness of the interphase as compared with the diameter of the fiber, or nonuniform thickness, even more elements will be needed in the finite element method model. Thus, using finite elements based on the elasticity theory for the modeling of interphases can be costly and inefficient.

The boundary element method has been demonstrated to be a viable alternative to the finite element method due to its features of boundary-only discretization and high accuracy in stress analysis, especially in fracture analysis (see, e.g., [15–18]). For the analysis of micromechanical behaviors of fiber-reinforced composites using the boundary element method, there are very few publications in the literature, and all of the boundary element method models developed so far are two-dimensional ones based on perfect-bonding or spring-like interface conditions. No boundary element method models have been attempted earlier to model the interphases directly as an elastic region between the fiber and matrix.

Achenbach and Zhu [2] developed a two-dimensional model of

[1]To whom correspondence should be addressed.

Contributed by the Applied Mechanics Division of THE AMERICAN SOCIETY OF MECHANICAL ENGINEERS for publication in the ASME JOURNAL OF APPLIED MECHANICS. Manuscript received by the ASME Applied Mechanics Division, Sept. 23, 1998; final revision, Sept. 23, 1999. Associate Technical Editor: W. K. Liu. Discussion on the paper should be addressed to the Technical Editor, Professor Lewis T. Wheeler, Department of Mechanical Engineering, University of Houston, Houston, TX 77204-4792, and will be accepted until four months after final publication of the paper itself in the ASME JOURNAL OF APPLIED MECHANICS.

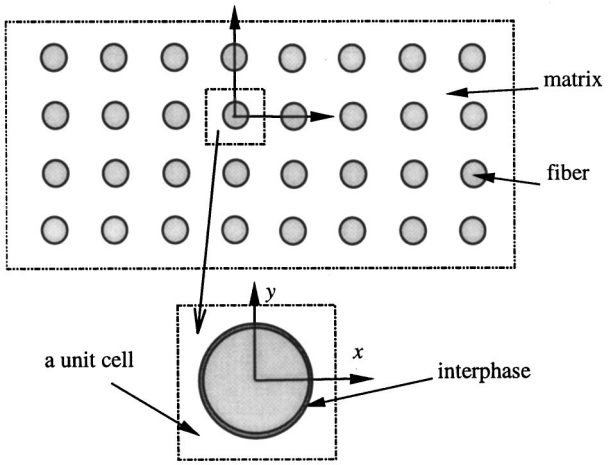

Fig. 1 The interphase in a fiber-reinforced composite

a square unit cell using the boundary element method. To study the effect of the interphase, the continuity of the tractions across the interface of fiber and matrix is maintained, while a linear relation between the displacement differences and the tractions across the interface is introduced. This simple relation represents a spring-like model of the interphase. The proportionality constants used in this model characterize the stiffness of the interphase. Based on this model, it was shown that the variations of the interphase parameters can cause pronounced changes in the stress distributions in the fiber and matrix. The initiation, propagation and arrest of the interface cracks were also analyzed. The same approach to the interphase modeling was extended in [3] to study hexagonal-array fiber composites, and in [4] to study the micromechanical behaviors of a cluster of fibers. Oshima and Watari [19] calculated the transverse effective Young's modulus using a two-dimensional boundary element method for a square unit cell model. No interphase was modeled and perfect bonding between the fiber and the matrix was assumed. Nevertheless, the boundary element method results using constant elements were shown to be in very good agreement with the experimental data. Gulrajani and Mukherjee [20] studied the sensitivities and optimal design of composites with a hexagonal array of fibers. A two-dimensional boundary element method model with the same spring-like interphase model as in [2] was used. The sensitivities of stresses at the interphase were calculated and employed to optimize the value of the stiffness of an interphase in order to minimize the possibility of failure of a composite. Most recently, Pan, Adams, and Rizzo [21] developed a similar two-dimensional boundary element method model using the same interphase relation as in [2] to study the perfectly bonded as well as imperfectly bonded fiber-reinforced composites. A main component in this research was the development of a library of Green's functions (or matrices of boundary element method equations) for analyzing fiber-reinforced composite materials, which can be used by engineers in the design of such composites. Although successful to some extent, all the above boundary element method models of the unit cells for fiber-reinforced composites with the spring-like interphase relations are incapable of providing other important information about the properties of composites, such as effects of changes of the thickness and nonuniform distribution of the interphases. Furthermore, in order to avoid overlapping of the fiber and matrix in the spring-like model, an iteration approach is needed. A trial calculation needs to be done first to check the sign of the normal traction at the interface. If the spring is in compression, continuity of the normal displacement is resumed and the boundary element method is applied again. This procedure is inefficient and can be costly. An improved boundary element method model of the interphases based on elasticity theory is desirable.

Interphases, as in fiber-reinforced composites, are thin shell-like structures. For this class of structures, there have been two major concerns in applying the boundary element method. The first concern is whether or not the conventional boundary integral equation for elasticity can be applied successfully to thin structures. It is well known in the boundary integral equation/boundary element method literature that the conventional boundary integral equation will degenerate when it is applied to cracks or thin voids in structures because of the closeness of the two crack surfaces (see, e.g., [16] and [22]). One of the remedies to such degeneracy in the conventional boundary integral equation for crack-like problems (*exterior-like* problems), is to employ the hypersingular boundary integral equation (see, e.g., [18,23–25]). Does this degeneracy occur when the conventional boundary integral equation is applied to thin structures (*interior-like* problems), such as thin shells? It was not clear in the boundary element method literature and the boundary element method based on elasticity had been avoided in analyzing thin shell-like structures for a long time due to this concern. Recently, it was shown in [26] and [27], both analytically and numerically, that the conventional boundary integral equation will not degenerate, contrary to the case of crack-like problems, when it is applied to thin shell-like structures if the displacement boundary conditions are not imposed at all the boundaries. Further discussions on this nondegeneracy issue for the boundary element method applied to shell-like structures can be found in [26] and [28]. Based on these new results, the degeneracy issue should no longer be a concern when the conventional boundary integral equation is applied to thin structures, once the second concern, that is, the numerical difficulty is addressed.

The numerical difficulty in the boundary integral equation is the nearly singular integrals which arise in thin structures when two parts of the boundary become close to each other. Detailed studies on the behaviors of the nearly singular integrals and comprehensive reviews of the earlier work in this regard can be found in [29] and [30]. One of the most efficient and accurate approaches to deal with the nearly singular integrals in the boundary element method for three-dimensional problems is to transform these (surface) integrals to line integrals analytically before the numerical integration ([22,26,31]). A similar approach can be established for two-dimensional elasticity problems ([27]). It has been demonstrated in [27] that very accurate numerical solutions can be obtained for thin structures with the thickness-to-length ratio in the micro and even nanoscales, using the newly developed boundary element method approach, without seeking refinement of the meshes as the thickness decreases.

Once the degeneracy issue for the conventional boundary integral equation in thin structure problems has been clarified and the nearly singular integrals can be dealt with accurately and efficiently, it is believed that the boundary element method can now be applied to a wide range of engineering problems, including simulations of thin shell-like structures ([26]) thin-film, and coatings in the micro or nanoscales ([27]) and in particular, the interphases in fiber-reinforced composite materials.

In this paper, detailed two-dimensional models for the interphases in fiber-reinforced composite materials have been developed based on the elasticity theory to study their micromechanical behaviors under transverse loading. All the regions—the fiber, matrix, and interfacial zone contained in a unit cell, are modeled using the advanced two-dimensional boundary element method with thin-body capabilities ([27]) and extended to multidomain cases. The interphases can have uniform thickness of any arbitrarily small values or nonuniform thickness. Interface stresses in the interphases and effective elastic moduli in the transverse directions are computed using this approach. This two-dimensional model of the interphases can provide more accurate interface stresses and therefore a more accurate account on the micromechanical behaviors of fiber-reinforced composites than the current spring-like models in the boundary element method literature.

2 The Boundary Element Method Formulation

For the unit cell models under transverse loading (Fig. 2), the following boundary integral equation for two-dimensional elasticity problems can be applied in each material domain (index notation is used in this section, where repeated subscripts imply summation):

$$C_{ij}(P_0)u_j^{(\beta)}(P_0)=\int_S [U_{ij}^{(\beta)}(P,P_0)t_j^{(\beta)}(P)-T_{ij}^{(\beta)}(P,P_0) \times u_j^{(\beta)}(P)]dS(P), \quad (1)$$

in which $u_i^{(\beta)}$ and $t_i^{(\beta)}$ are the displacement and traction fields, respectively; $U_{ij}^{(\beta)}(P,P_0)$ and $T_{ij}^{(\beta)}(P,P_0)$ the displacement and traction kernels (Kelvin's solution or the fundamental solution), respectively; P the field point and P_0 the source point; and S the boundary of the single material domain, (Fig. 2). $C_{ij}(P_0)$ is a constant coefficient matrix depending on the smoothness of the curve S at the source point P_0 (e.g., $C_{ij}(P_0)=1/2\delta_{ij}$ if S is smooth at point P_0, where δ_{ij} is the Kronecker delta). The superscript β on the variables in Eq. (1) signifies the dependence of these variables on the material domains, as specified below:

$$\beta=f: \quad \text{fiber domain} \quad (S=S_1);$$

$$\beta=i: \quad \text{interphase domain} \quad (S=S_1\cup S_2);$$

$$\beta=m: \quad \text{matrix domain} \quad (S=S_2\cup S_3).$$

The two kernel functions $U_{ij}^{(\beta)}(P,P_0)$ and $T_{ij}^{(\beta)}(P,P_0)$ in boundary integral equation (1) are given as follows for plane-strain problems:

$$U_{ij}^{(\beta)}(P,P_0)=\frac{1}{8\pi\mu^{(\beta)}(1-\nu^{(\beta)})}\left[(3-4\nu)\delta_{ij}\ln\left(\frac{1}{r}\right)+r_{,i}r_{,j}\right],$$

$$T_{ij}^{(\beta)}(P,P_0)=-\frac{1}{4\pi(1-\nu^{(\beta)})}\frac{1}{r}\{r_{,n}[(1-2\nu^{(\beta)})\delta_{ij}+2r_{,i}r_{,j}] +(1-2\nu^{(\beta)})(r_{,j}n_i-r_{,i}n_j)\}, \quad (2)$$

where $\mu^{(\beta)}$ is the shear modulus and $\nu^{(\beta)}$ the Poisson's ratio for the three different domains, respectively; r the distance from the source point P_0 to the field point P; n_i the directional cosines of the outward normal n; and $(),_i=\partial()/\partial x_i$ with x_i being the coordinates of the field point P.

In Eq. (1) the integral containing the $U_{ij}^{(\beta)}(P,P_0)$ kernel is weakly singular, while the one containing $T_{ij}^{(\beta)}(P,P_0)$ is strongly singular and must be interpreted in the Cauchy principal value sense. There is a vast body of literature on how to deal with the Cauchy principle value integrals in the boundary element method formulations for bulky-shaped structures, either analytically for some special cases or numerically for other cases. An alternative approach is to transform the boundary integral equation in the form of Eq. (1) into a weakly singular form by using some simple solutions or integral identities for the fundamental solution ([32,33]), before doing any numerical work. However, when the structure becomes thin in shape, such as the interphase shown in Fig. 2, both integrals in Eq. (1) are difficult to deal with when the source point is on one side and the integration is carried out on the other side of the thin structure. These types of integrals are called nearly singular integrals since the distance r is very small in this case but is still not zero. Most techniques for dealing with the singular integrals do not work for nearly singular integrals and special attention is needed. Recently, several techniques, including singularity subtractions, analytical integration, and nonlinear coordinate transformations have been developed for the two-dimensional elasticity boundary integral equation to calculate the nearly singular integrals arising in thin structures ([27]). The combination of these techniques is found to be extremely effective and efficient in computing the nearly singular integrals in the two-dimensional boundary integral equation, no matter how close the source point is to the element of integration. Very accurate boundary element method results have been obtained using this approach for thin structures, such as coatings on macroscale structures, with the coating thickness-to-length ratios in the micro to nanoscales and with a small number of boundary elements. The same approach in [27] is applied in this paper to compute the nearly singular integrals arising in the modeling of the interphases.

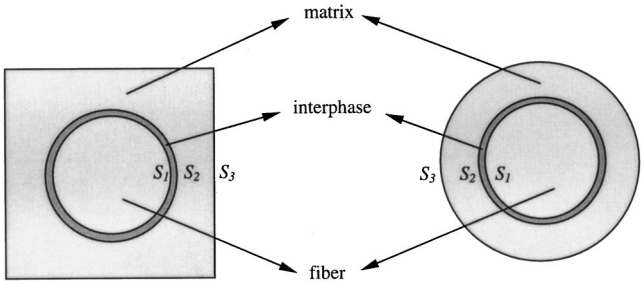

Fig. 2 Two unit cell models of the fiber-interphase-matrix system

Employing the boundary elements (line elements in two-dimensional) on the boundary and interfaces S_1, S_2, and S_3, the discretized equations of the three boundary integral equations as given in (1) for the fiber, interphase, and matrix can be written as follows (cf., e.g., [17]):

$$\mathbf{T}_1^{(f)}\mathbf{u}_1^{(f)}=\mathbf{U}_1^{(f)}\mathbf{t}_1^{(f)}, \quad \text{(in fiber domain)} \quad (3)$$

$$\mathbf{T}_1^{(i)}\mathbf{u}_1^{(i)}+\mathbf{T}_2^{(i)}\mathbf{u}_2^{(i)}=\mathbf{U}_1^{(i)}\mathbf{t}_1^{(i)}+\mathbf{U}_2^{(i)}\mathbf{t}_2^{(i)}, \quad \text{(in interphase domain)} \quad (4)$$

$$\mathbf{T}_2^{(m)}\mathbf{u}_2^{(m)}+\mathbf{T}_3^{(m)}\mathbf{u}_3^{(m)}=\mathbf{U}_2^{(m)}\mathbf{t}_2^{(m)}+\mathbf{U}_3^{(m)}\mathbf{t}_3^{(m)}, \quad \text{(in matrix domain)} \quad (5)$$

in which $\mathbf{U}$ and $\mathbf{T}$ are matrices generated from the $U_{ij}^{(\beta)}(P,P_0)$ and $T_{ij}^{(\beta)}(P,P_0)$ kernels, respectively; $\mathbf{u}$ and $\mathbf{t}$ the displacement and traction vectors, respectively. The superscripts indicate the material domain, while the subscripts indicate the interface or boundary (S_1, S_2, or S_3) on which the integration is performed.

Assuming perfect bonding at the fiber/interphase (S_1) and interphase/matrix (S_2) interfaces, one can write the following interface conditions:

$$\text{On } S_1: \quad \mathbf{u}_1^{(f)}=\mathbf{u}_1^{(i)}\equiv\mathbf{u}_1, \quad \text{(continuity)} \quad (6)$$

$$\mathbf{t}_1^{(f)}=-\mathbf{t}_1^{(i)}\equiv\mathbf{t}_1, \quad \text{(equilibrium)} \quad (7)$$

$$\text{On } S_2: \quad \mathbf{u}_2^{(i)}=\mathbf{u}_2^{(m)}\equiv\mathbf{u}_2, \quad \text{(continuity)} \quad (8)$$

$$\mathbf{t}_2^{(i)}=-\mathbf{t}_2^{(m)}\equiv\mathbf{t}_2, \quad \text{(equilibrium)} \quad (9)$$

where $\mathbf{u}_1$, $\mathbf{t}_1$, $\mathbf{u}_2$, and $\mathbf{t}_2$ are defined as the interface displacement or traction vectors.

Applying the interface conditions (6)–(9) in Eqs. (3)–(5), one obtains the following system:

$$\begin{bmatrix} \mathbf{T}_1^{(f)} & \mathbf{0} & \mathbf{0} \\ \mathbf{T}_1^{(i)} & \mathbf{T}_2^{(i)} & \mathbf{0} \\ \mathbf{0} & \mathbf{T}_2^{(m)} & \mathbf{T}_3^{(m)} \end{bmatrix} \begin{Bmatrix} \mathbf{u}_1 \\ \mathbf{u}_2 \\ \mathbf{u}_3 \end{Bmatrix} = \begin{bmatrix} \mathbf{U}_1^{(f)} & \mathbf{0} & \mathbf{0} \\ -\mathbf{U}_1^{(i)} & \mathbf{U}_2^{(i)} & \mathbf{0} \\ \mathbf{0} & -\mathbf{U}_2^{(m)} & \mathbf{U}_3^{(m)} \end{bmatrix} \begin{Bmatrix} \mathbf{t}_1 \\ \mathbf{t}_2 \\ \mathbf{t}_3 \end{Bmatrix},$$

where $\mathbf{u}_3\equiv\mathbf{u}_3^{(m)}$ and $\mathbf{t}_3\equiv\mathbf{t}_3^{(m)}$ have been used for simplicity. Rearranging the columns and moving all the (unknown) interface variables to the left-hand side, one finally arrives at

$$\begin{bmatrix} \mathbf{T}_1^{(f)} & -\mathbf{U}_1^{(f)} & \mathbf{0} & \mathbf{0} & \mathbf{0} \\ \mathbf{T}_1^{(i)} & \mathbf{U}_1^{(i)} & \mathbf{T}_2^{(i)} & -\mathbf{U}_2^{(i)} & \mathbf{0} \\ \mathbf{0} & \mathbf{0} & \mathbf{T}_2^{(m)} & \mathbf{U}_2^{(m)} & \mathbf{T}_3^{(m)} \end{bmatrix} \begin{Bmatrix} \mathbf{u}_1 \\ \mathbf{t}_1 \\ \mathbf{u}_2 \\ \mathbf{t}_2 \\ \mathbf{u}_3 \end{Bmatrix} = \begin{bmatrix} \mathbf{0} \\ \mathbf{0} \\ \mathbf{U}_3^{(m)} \end{bmatrix} \{\mathbf{t}_3\}. \tag{10}$$

The last column in the matrix on the left-hand side and the matrix on the right-hand side may need to be rearranged again according to the boundary conditions specified on S_3.

Equation (10) is the global system of equations for the fiber-interphase-matrix model. The system has a banded matrix due to the multidomain nature of the problem. This system of equations satisfies both the continuity and equilibrium conditions at the interfaces explicitly, which is an advantage of the boundary element method approach over the finite element method in which only the continuity of displacement fields can be satisfied explicitly. By solving Eq. (10), one can obtain the displacements and tractions at the two interfaces and the boundary, and then calculate the interface stresses based on the traction and displacement fields.

3 Two Unit Cell Models With the Interphase

Two unit cell models are used in this paper, namely, the concentric cylinder model and the square model (see, e.g., [12]) both of which include the interphase (Fig. 2). For the cylinder model, analytical solutions are obtained for the displacement and stress fields, which can be employed to validate the boundary element method results. For the square model, many finite element and boundary element solutions are available in the literature for the effective elastic moduli which will be compared with the data from the present boundary element method approach.

3.1 Concentric Cylinder Model. For the concentric cylinder model, Fig. 3, the response of the composite in the x-y plane is axisymmetric if the applied load or displacement on the boundary S_3 is also axisymmetric. Here it is assumed that a radial displacement δ is given on S_3 (at $r=c$, Fig. 3). Applying the theory of elasticity for plane strain case in the polar coordinate system (r,θ), one can derive the following expressions for the radial displacement and stress fields in the fiber, interphase, and matrix, respectively (see the Appendix for details):

$$\begin{aligned} u^{(f)}(r) &= A^{(f)} r, \quad (0 \leqslant r \leqslant a) \\ u^{(i)}(r) &= A^{(i)} r + \frac{B^{(i)}}{r}, \quad (a \leqslant r \leqslant b) \\ u^{(m)}(r) &= A^{(m)} r + \frac{B^{(m)}}{r}, \quad (b \leqslant r \leqslant c) \end{aligned} \tag{11}$$

and

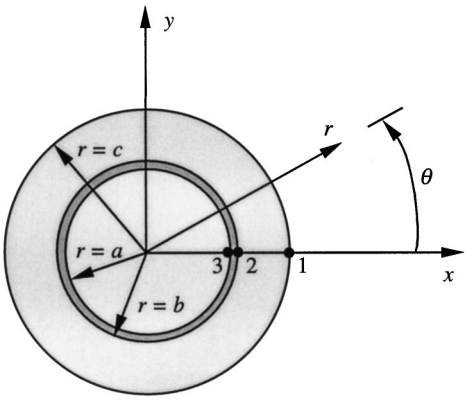

Fig. 3 Concentric cylindrical model

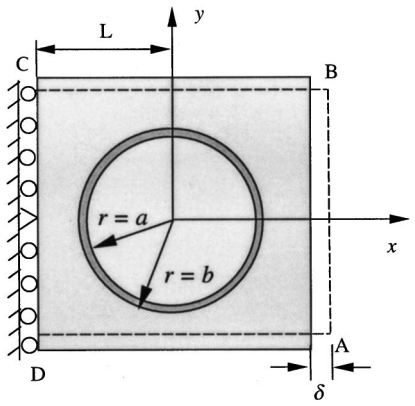

Fig. 4 Square model under tension

$$\begin{aligned} \sigma_r^{(f)} &= \sigma_\theta^{(f)} = k^{(f)} A^{(f)}, \quad (0 \leqslant r \leqslant a) \\ \sigma_r^{(i)} &= k^{(i)} \left[A^{(i)} - (1-2\nu^{(i)}) \frac{B^{(i)}}{r^2} \right], \\ \sigma_\theta^{(i)} &= k^{(i)} \left[A^{(i)} + (1-2\nu^{(i)}) \frac{B^{(i)}}{r^2} \right], \quad (a \leqslant r \leqslant b) \\ \sigma_r^{(m)} &= k^{(m)} \left[A^{(m)} - (1-2\nu^{(m)}) \frac{B^{(m)}}{r^2} \right], \\ \sigma_\theta^{(m)} &= k^{(m)} \left[A^{(m)} + (1-2\nu^{(m)}) \frac{B^{(m)}}{r^2} \right], \quad (b \leqslant r \leqslant c) \end{aligned} \tag{12}$$

where the constants $A^{(\beta)}$, $B^{(\beta)}$, and $k^{(\beta)}$ ($\beta = f$, i and m) are given in the Appendix.

From the above expressions, one can compute the radial displacement and stress components at any point in the three domains within the cylinder model for any small values of the interphase thickness.

3.2 Square Model. As shown in Fig. 4, the boundary conditions for the square model under *tension* are

$$\begin{aligned} &\text{along } AB: \quad u_x = \delta, \quad t_y = 0; \\ &\text{along } BC: \quad u_y = -C_0, \quad t_x = 0; \\ &\text{along } CD: \quad u_x = 0, \quad t_y = 0, \\ &\text{except at } y = 0 \text{ where } u_x = u_y = 0; \\ &\text{along } DA: \quad u_y = C_0, \quad t_x = 0; \end{aligned} \tag{13}$$

where u_x, u_y, t_x, and t_y are the displacement and traction components, respectively; δ the given displacement (Fig. 4); and C_0 an unknown constant. This unknown constant is meant to keep the edges BC and DA straight after the deformation. This represents the constraint of the neighboring cells to the one under study. In the literature, there are several ways in dealing with these subtle boundary conditions along the top and bottom edges. For example, in [9] C_0 is chosen as zero in one case and nonzero in another case. This is equivalent to another given displacement condition besides the one imposed along the two vertical edges. In [2] and recently in [21], C_0 is regarded as an unknown and the condition $\int_{-L}^{L} \sigma_y dx = 0$ along the top or bottom edges is used to provide the additional equation needed for solving this unknown together with other unknown boundary variables. Discretization of this simple equation using shape functions is needed. In [19], however, this straight-line constraint is totally ignored, and $t_x = t_y = 0$ (traction-free conditions) are assumed. It is found that results for the unit cell model is not very sensitive to all the different techniques mentioned above. In this paper, C_0 is as-

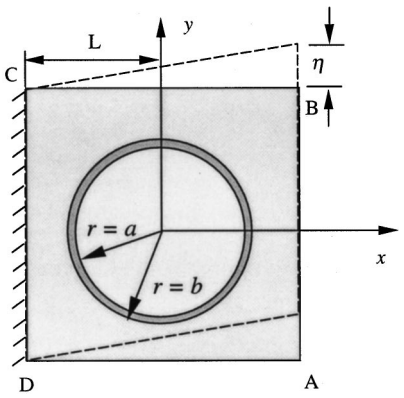

Fig. 5 Square model under shear deformation

sumed to be unknown, but a different approach is employed to enforce the straight-line condition, instead of solving for this unknown constant with additional equations. Here the penalty method used in the finite element method for multipoint constraints (see, e.g., [34]) is introduced in the boundary element method equations to enforce that all the nodes along edges BC and DA remain along straight lines after deformation. To implement this penalty method in the boundary element method equations a very large number (penalty) with a proper sign is placed in the locations in the matrix corresponding to the related displacement components. Then these displacement components will have the same value after the system of equations is solved. It is very easy to implement this penalty method in the boundary element method equations and no additional equation is needed.

Once stresses on the boundary are determined, the average tensile stress along the edge AB is evaluated by

$$\overline{\sigma_x}=\frac{1}{2L}\int_{-L}^{L}\sigma_x(L,y)dy. \tag{14}$$

The effective Young's modulus in the transverse direction and under the *plane-strain* condition is thus determined by

$$E_x'=\frac{\overline{\sigma_x}}{\overline{\varepsilon_x}}=\frac{\int_{-L}^{L}\sigma_x(L,y)dy}{\delta}, \tag{15}$$

where $\overline{\epsilon_x}=\delta/2L$ is the average tensile strain. The effective Poisson's ratio under the *plane-strain* condition can be determined by

$$v_{xy}'=-\frac{\overline{\varepsilon_y}}{\overline{\varepsilon_x}}, \tag{16}$$

in which $\overline{\varepsilon_y}$ is the average strain in the *y*-direction.

For the square model under *shear* deformation, Fig. 5, the boundary conditions are

$$\begin{aligned}&\text{along } AB: \quad u_x=0,\ u_y=\eta;\\ &\text{along } BC: \quad u_x=0,\ t_y=0;\\ &\text{along } CD: \quad u_x=0,\ u_y=0;\\ &\text{along } DA: \quad u_x=0,\ t_y=0.\end{aligned} \tag{17}$$

The average shear stress along edge AB can be evaluated by

$$\overline{\tau_{xy}}=\frac{1}{2L}\int_{-L}^{L}\tau_{xy}(L,y)dy, \tag{18}$$

and the effective shear modulus in the transverse plane and under the *plane-strain* condition is

$$G_{xy}'=\frac{\overline{\tau_{xy}}}{\overline{\gamma_{xy}}}=\frac{\int_{-L}^{L}\tau_{xy}(L,y)dy}{\eta}, \tag{19}$$

where $\overline{\gamma_{xy}}=\eta/2L$ is the average shear strain.

Finally, one recognizes that the material constants E_x', ν_{xy}', and G_{xy}' given in Eqs. (15), (16), and (19), respectively, are determined under the *plane-strain* condition which accounts for the constraint in the *z*-direction ($\varepsilon_z=0$). These constants are related to the intrinsic material properties by the following relations (cf., e.g., [35] and [21]):

$$E_x=\frac{1+2\nu_{xy}'}{(1+\nu_{xy}')^2}E_x',\quad \nu_{xy}=\frac{\nu_{xy}'}{1+\nu_{xy}'},\quad G_{xy}=G_{xy}', \tag{20}$$

which are the effective Young's modulus, Poisson's ratio, and shear modulus, respectively, in the transverse direction for the composite.

4 Numerical Examples

4.1 Cylinder Model. The cylinder model (Fig. 3) is studied first to validate the developed boundary element method formulation and the solution strategy, since for this idealized geometry the analytical solutions are available (see Eqs. (11)–(12) and the Appendix). The specified radial displacement on the boundary (at $r=c$) is δ. The following material constants for a glass/epoxy composite are used:

$$\begin{aligned}&\text{for fiber:} \quad E^{(f)}=72.4\ \text{GPa}\ (10.5\times10^6\ \text{psi}),\ \nu^{(f)}=0.22;\\ &\text{for interphase:} \quad E^{(i)}=36.2\ \text{GPa}\ (5.25\times10^6\ \text{psi}),\ \nu^{(i)}=0.30;\\ &\text{for matrix:} \quad E^{(m)}=3.45\ \text{GPa}\ (0.5\times10^6\ \text{psi}),\ \nu^{(m)}=0.35;\end{aligned}$$

where the Young's modulus of the interphase has been taken as half of that of the fiber; and the dimensions used are

$$a=c/2,\quad b=a+h,$$

with *h* being the thickness of the interphase, which is varying.

Quadratic line elements are employed in the discretization and two meshes are tested, one with 24 elements (eight on each circle) and another one with 48 elements (16 on each circle). Differences

Table 1 Results of the radial displacement $u(\times10^{-2}\delta)$ for the cylinder model

	$h=0.1a$		$h=0.01a$		$h=0.001a$	
	Point 2	Point 3	Point 2	Point 3	Point 2	Point 3
BEM	8.2961	7.0833	6.7379	6.6225	6.5909	6.5794
Analytical	8.2958	7.0830	6.7378	6.6224	6.5925	6.5810
Error (%)	0.0036	0.0042	0.0015	0.0015	0.0243	0.0243

Table 2 Results of the radial stress $\sigma_r(\times E^{(m)}\delta/c)$ for the cylinder model

	$h=0.1a$			$h=0.01a$			$h=0.001a$		
	Point 1	Point 2	Point 3	Point 1	Point 2	Point 3	Point 1	Point 2	Point 3
BEM	3.6515	4.2806	4.3550	3.4215	4.0636	4.0714	3.4009	4.0442	4.0449
Analytical	3.6513	4.2803	4.3544	3.4214	4.0633	4.0711	3.4006	4.0461	4.0458
Error (%)	0.0055	0.0070	0.0138	0.0029	0.0074	0.0074	0.0088	0.0470	0.0222

in the results from the two meshes are less than five percent and the results from the refined mesh (48 elements) are reported. The radial displacements and stresses at selected points (Fig. 3) are given in Table 1 and Table 2, respectively. It is observed that the maximum errors of the displacement and stress using the developed boundary element method are less than 0.05 percent in all the cases with different thickness of the interphase. These results demonstrate that the developed boundary element method approach is extremely accurate and effective in modeling the interphases with any small thickness, as has been confirmed in the context of single material problems ([27]).

4.2 Square Model

(a) Calculation of Effective Young's Modulus With Varying Interphase Property. First, the square model under a stretch in the *x*-direction is considered (Fig. 4). The properties of the constituent materials considered are

$$\text{for fiber:} \quad E^{(f)}=84.0 \text{ GPa}, \quad \nu^{(f)}=0.22;$$

$$\text{for interphase:} \quad E^{(i)}=4.0\sim 12.0 \text{ GPa}, \quad \nu^{(i)}=0.34;$$

$$\text{for matrix:} \quad E^{(m)}=4.0 \text{ GPa}, \quad \nu^{(m)}=0.34;$$

and, $a=8.5\ \mu$m, $b=a+h$, $2L=21.31\ \mu$m (fiber volume fraction $V_f=50$ percent). Young's modulus for the interphase is changing in the range between 4.0 and 12.0 GPa. The effect of the variations in the interphase material on the effective Young's modulus of the composite is of the primary interest here. A total of 64 quadratic boundary elements are used, with 16 elements on each of the two circular interfaces and 32 elements on the outer boundary. Table 3 shows the effective Young's moduli obtained from the boundary element method stress data using Eq. (15) and then Eq. (20), and compared with those from the finite element method quarter model with 3518 linear triangular elements in [9] for the thickness $h=1.0\ \mu$m. The boundary element method results are slightly lower than those from the finite element method data. This may be caused by the use of linear triangular element in the finite element method which tends to overestimate the stiffness of the structure. It is noticed that the different boundary conditions along the top and bottom edges of the square model (free-traction or straight-line conditions) have very little influences on the final effective Young's modulus. It should also be pointed out that for the finite element results in [9], the only thickness considered is $h=1.0\ \mu$m which is relatively large compared with the fiber radius ($a=8.5\ \mu$m). If a smaller thickness were used in the finite element model, a much larger number of elements would have been needed in order to avoid large aspect ratios in the finite element mesh, as demonstrated in a similar study (see [27]). However, for the boundary element method employed here, the same number of elements can be used no matter how small the thickness of the interphase is.

(b) Effect of the Interphase Thickness. Figure 6 shows the effect of different interphase thicknesses to the effective Young's modulus. In order to compare with the data in [21] and [19], the same material constants as listed in Section 4.1 (for the cylinder model) are used. It is found that the effect of the thickness is not significant on the effective Young's moduli when the fiber volume fraction V_f is small (50 percent and less), while significant effect is observed when V_f is large (70 percent). This may be due to the fact that the effective elastic moduli are obtained by evaluating the average stress on the outer boundary of the matrix (edge AB, Fig. 4). When the fiber volume fraction is small, the interphase is away from the matrix outer boundary and thus changing the interphase thickness does not considerably affect the stresses on the edge AB. This will change if the fiber volume fraction is large (e.g., 70 percent) when the interphase becomes closer to the outer boundary of the matrix. It should also be pointed out that when the fiber volume fraction is large, it will present additional difficulty in the modeling using the finite element method and earlier boundary element method formulation, because of the thinness of the matrix region. However, for the current boundary element method formulation, this additional thinness of the matrix domain does not present any problem.

(c) Effect of Nonuniform Thickness. Next, the effect of nonuniform thickness of the interphase on the interface stresses and effective elastic moduli is investigated. The starting model (Fig. 4) is the same as the one used for Table 3 with the material constants listed at the beginning of this subsection (with $E^{(i)}=42.0$ GPa). To form the nonuniform distribution of the interphase, the outer boundary of the interphase is shifted to the left

Table 3 Effective transverse elastic modulus (GPa) using the square unit cell model

Interphase property $E^{(i)}$ (GPa)	*Current BEM with traction-free conditions on BC and DA*	*Current BEM with straight-line conditions on BC and DA*	*FEM* ([9])
4.0	11.61	11.61	12.25
6.0	13.18	13.02	13.71
8.0	13.97	13.89	14.68
12.0	15.04	14.93	15.91

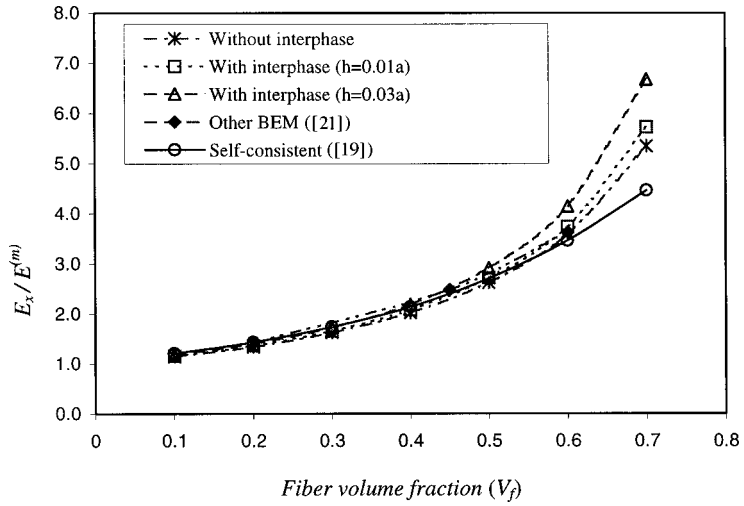

Fig. 6 Influence of the thickness on the effective Young's modulus

slightly (see Fig. 7). When the offset Δ is close to h (the initial, uniform thickness), the change of the interphase thickness in the x-direction is the largest ($\Delta = 0$ corresponds to the uniform interphase). The interface normal stresses at points 1 and 2 (Fig. 7), normalized by those in the uniform case, are plotted in Fig. 8. Due to the misalignment of the fiber and interphase centers, the interface stress at point 1 (which is the maximum interface normal stress) increases for about 50 percent while the stress at point 2 (the second largest interface stress) increases for about 30 percent. However, the effect of the nonuniform thickness of the interphase on the effective Young's modulus is found to be less than three percent. This, again, is largely due to the averaging process on the edge AB which is away from the interphase.

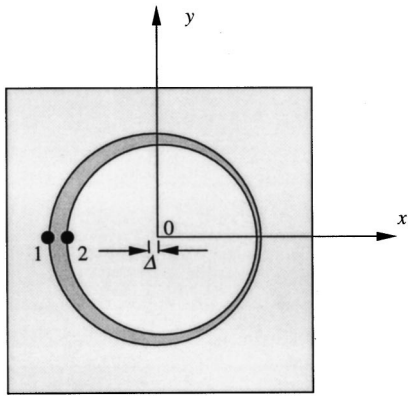

Fig. 7 The interphase with nonuniform thickness

(d) Calculation of Shear Modulus With Varying Interphase Thickness. Finally, the effective shear modulus in the transverse direction is calculated using the square unit cell model shown in Fig. 5. The boundary conditions applied are listed in (17) and Eqs. (19)–(20) are used to compute the shear modulus. In order to compare the results with those in the literature, the following materials properties for a Kevlar/epoxy composite are used in the current boundary element method calculation:

$$\text{for fiber:} \quad E^{(f)} = 7.0 \text{ GPa}, \quad \nu^{(f)} = 0.30;$$

$$\text{for interphase:} \quad E^{(i)} = 5.0 \text{ GPa}, \quad \nu^{(i)} = 0.35;$$

$$\text{for matrix:} \quad E^{(m)} = 3.0 \text{ GPa}, \quad \nu^{(m)} = 0.35.$$

Table 4 shows the results of the effective shear modulus by the current boundary element method with and without the presence of the interphase. The data without the interphase ($h = 0$) agrees very well with the results from the finite element method ([6]) and

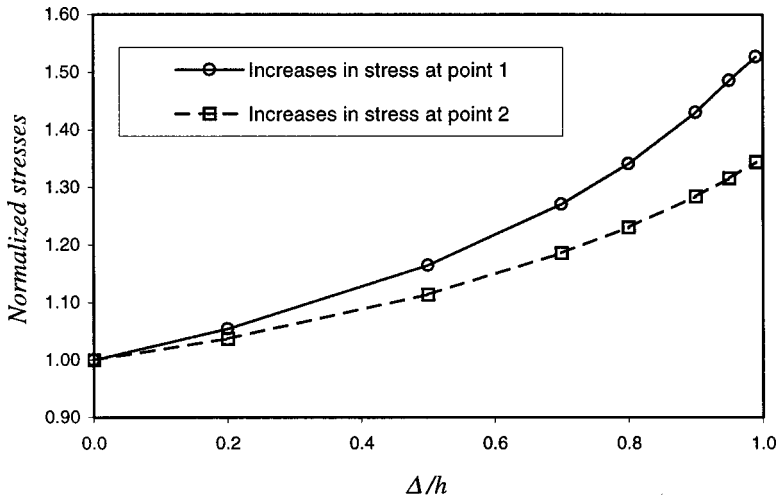

Fig. 8 Effect of nonuniform thickness on the interface stress

Table 4 Effective transverse shear modulus (GPA)

	Fiber volume fraction (V_f)			
	0.2	0.4	0.6	0.7
FEM ([6])	1.297	1.529	1.826	---
Other BEM ([21])	1.294	1.513	1.798	---
Current BEM ($h = 0.0$)	1.2939	1.5133	1.7981	1.9866
Current BEM ($h = 0.001a$)	1.2941	1.5139	1.7994	1.9885
Current BEM ($h = 0.01a$)	1.2964	1.5196	1.8111	2.0059
Current BEM ($h = 0.1a$)	1.3205	1.5807	1.9446	---

the other boundary element method ([21]) both of which used the perfect bonding condition and did not model the interphase. With the increase of the thickness of the interphase, the shear modulus deviates from the perfect bonding case slightly, with the largest change (about eight percent) occurring at the fiber volume fraction $V_f = 0.6$, for the interphase property considered. When $V_f = 0.7$ and $h = 0.1a$, the interphase will be outside the boundary of the unit cell. This is not permissible and thus no boundary element method data are generated.

5 Conclusion

The advanced boundary element method formulation with thin-body capabilities for elastostatic problems has been extended to multidomain problems and applied to model the interphases in fiber-reinforced composites under transverse loading. Compared with the current spring-like models for the interphases in the boundary element method literature, this new interphase model is based on the elasticity theory and thus provides a more accurate account of the interphases in fiber-reinforced composites within the linear theory. The developed boundary element code using the object-oriented programming language (C++) can be utilized in analyzing the micromechanical properties of fiber-reinforced composites with the presence of interphases of any arbitrarily small thickness (uniform or nonuniform). The approach is very accurate as is validated using the concentric cylinder model for which the analytical solution has been derived. It is also very efficient as only a small number (less than one hundred) of boundary elements are needed to model a *whole* unit cell for the boundary element analysis, compared with the large number (more than a few thousands) of finite elements often needed for a *quarter* model in the finite element method analysis. The approach provides a greater flexibility in parametric study of the interphases as well, since the geometry, size, or material property of the interphases can be changed very easily to investigate their effect on the micromechanical behaviors of the fiber-reinforced composites.

Numerical studies in this paper show that the thickness, nonuniform distribution, and material property of the interphase can have significant influences on the micromechanical behaviors of the composites, such as effective elastic moduli and interface stresses, especially when the fiber volume fractions are large. These observations are consistent with the findings in both the finite element method and boundary element method literatures on this subject.

Considerations of interface cracks in the present boundary element model and extension of the boundary element code to three dimensions to study the fiber-pullout failure modes will be interesting and challenging next steps, both of which will further demonstrate the robustness of the developed boundary element method approach as compared with the finite element method or previous boundary element method approaches to the micromechanical analysis of fiber-reinforced composites.

Acknowledgment

Support of this research by the National Science Foundation under the grant CMS 9734949 is gratefully acknowledged. The first author would like to thank Prof. Frank Rizzo at Iowa State University and Dr. Lingyun Pan at Caterpillar, Inc. for many discussions and help on this project.

Appendix

Analytical Solution for the Concentric Cylinder Model. Here the analytical solution for the concentric cylinder model used to validate the boundary element method results is derived. For the concentric cylinders, the response of the composite is axisymmetric. Thus the equilibrium equation for two-dimensional elasticity in the polar coordinate system reduces to

$$\frac{d\sigma_r}{dr} + \frac{1}{r}(\sigma_r - \sigma_\theta) = 0, \tag{A1}$$

where the stress components $(\sigma_r, \sigma_\theta)$ are functions of r only, and the shearing stress $\tau_{r\theta}$ is zero. The stress-strain relations for the plane-strain case are

$$\sigma_r = \frac{E}{(1+\nu)(1-2\nu)}[(1-\nu)\varepsilon_r + \nu\varepsilon_\theta],$$

$$\sigma_\theta = \frac{E}{(1+\nu)(1-2\nu)}[(1-\nu)\varepsilon_\theta + \nu\varepsilon_r]. \tag{A2}$$

The strain-displacement relations are

$$\varepsilon_\theta = \frac{u}{r}, \quad \varepsilon_r = \frac{du}{dr}. \tag{A3}$$

Equations (*A*1), (*A*2), and (*A*3) lead to the following equation for the radial displacement:

$$\frac{d^2u}{dr^2} + \frac{1}{r}\frac{du}{dr} - \frac{u}{r^2} = 0, \tag{A4}$$

where u is the displacement in the radial direction.

The solution of the above equation has the following form:

$$u(r) = Ar + \frac{B}{r}, \tag{A5}$$

in which A and B are determined by the applied boundary conditions. The above form of the solution is the general form which valid for the fiber, interphase, and matrix. Thus for the three domains, one has

$$u^{(f)}(r) = A^{(f)}r, \quad (\text{assume } B^{(f)} = 0) \quad (0 \leqslant r \leqslant a)$$

$$u^{(i)}(r) = A^{(i)}r + \frac{B^{(i)}}{r}, \quad (a \leqslant r \leqslant b)$$

$$u^{(m)}(r) = A^{(m)}r + \frac{B^{(m)}}{r}, \quad (b \leqslant r \leqslant c). \tag{A6}$$

If $B^{(f)} \neq 0$, then at $r = 0$, the displacement $u^{(f)}(0)$ will approach infinity, which is not warranted.

Boundary and interface conditions are

$$\begin{aligned} &\text{at } r = c, \quad u^{(m)}(c) = \delta, \\ &\text{at } r = b, \quad u^{(i)}(b) = u^{(m)}(b), \\ &\qquad\qquad \sigma_r^{(i)}(b) = \sigma_r^{(m)}(b), \\ &\text{at } r = a, \quad u^{(i)}(a) = u^{(f)}(a), \\ &\qquad\qquad \sigma_r^{(i)}(a) = \sigma_r^{(f)}(a), \end{aligned} \tag{A7}$$

where δ is the displacement applied on the outer boundary of the matrix.

Applying the relations (*A*2), (*A*3), and (*A*6) in the above five equations in (*A*7) from the boundary and interface conditions, one can find the five constants to be

$$A^{(m)}=\frac{c\,\delta\left[(1-2\nu^{(m)})-\dfrac{k^{(i)}}{k^{(m)}}M\right]}{b^2+(1-2\nu^{(m)})c^2+\dfrac{k^{(i)}}{k^{(m)}}(b^2-c^2)M},$$

$$B^{(m)}=c\,\delta-A^{(m)}c^2,$$

$$\text{and}\quad k^{(f)}=\frac{E^{(f)}}{(1+\nu^{(f)})(1-2\nu^{(f)})},\qquad k^{(i)}=\frac{E^{(i)}}{(1+\nu^{(i)})(1-2\nu^{(i)})},$$

$$k^{(m)}=\frac{E^{(m)}}{(1+\nu^{(m)})(1-2\nu^{(m)})},$$

$$M=\frac{a^2(1-2\nu^{(i)})(k^{(f)}-k^{(i)})+b^2[k^{(f)}+(1-2\nu^{(i)})k^{(i)}]}{a^2(k^{(f)}-k^{(i)})-b^2[k^{(f)}+(1-2\nu^{(i)})k^{(i)}]},$$

$$B^{(i)}=\frac{(b^2-c^2)A^{(m)}+c\,\delta}{1-\dfrac{b^2}{a^2}\dfrac{k^{(f)}+k^{(i)}(1-2\nu^{(i)})}{k^{(f)}-k^{(i)}}},$$

$$A^{(i)}=-\frac{B^{(i)}}{a^2}\frac{k^{(f)}+(1-2\nu^{(i)})k^{(i)}}{k^{(f)}-k^{(i)}},$$

$$A^{(f)}=A^{(i)}+\frac{B^{(i)}}{a^2}. \tag{A8}$$

These results, together with Eqs. (11)–(12), provide the analytical solutions of the displacement and stress for the cylinder model. Note that the solution is valid for any arbitrarily small thickness of the interphase and thus is very useful in validating the boundary element solutions. This solution can also be applied to other layered structures of cylindrical shapes, such as cables.

References

[1] Chawla, K. K., 1987, *Composite Materials: Science and Engineering*, Springer-Verlag, New York.

[2] Achenbach, J. D., and Zhu, H., 1989, ''Effect of Interfacial Zone on Mechanical Behavior and Failure of Fiber-Reinforced Composites,'' J. Mech. Phys. Solids, **37**, No. 3, pp. 381–393.

[3] Achenbach, J. D., and Zhu, H., 1990, ''Effect of Interphases on Micro and Macromechanical Behavior of Hexagonal-Array Fiber Composites,'' ASME J. Appl. Mech., **57**, pp. 956–963.

[4] Zhu, H., and Achenbach, J. D., 1991, ''Effect of Fiber-Matrix Interphase Defects on Microlevel Stress States at Neighboring Fibers,'' J. Compos. Mater., **25**, pp. 224–238.

[5] Hashin, Z., 1991, ''Composite Materials With Interphase: Thermoelastic and Inelastic Effects,'' *Inelastic Deformation of Composite Materials*, G. J. Dvorak, ed., Springer, New York, pp. 3–34.

[6] Yeh, J. R., 1992, ''The Effect of Interface on the Transverse Properties of Composites,'' Int. J. Solids Struct., **29**, pp. 2493–2505.

[7] Jasiuk, I., and Kouider, M. W., 1993, ''The Effect of an Inhomogeneous Interphase on the Elastic Constants of Transversely Isotropic Composites,'' Mech. Mater., **15**, pp. 53–63.

[8] Lagache, M., Agbossou, A., Pastor, J., and Muller, D., 1994, ''Role of Interphase on the Elastic Behavior of Composite Materials: Theoretical and Experimental Analysis,'' J. Compos. Mater., **28**, No. 12, pp. 1140–1157.

[9] Wacker, G., Bledzki, A. K., and Chate, A., 1998, ''Effect of Interphase on the Transverse Young's Modulus of Glass/Epoxy Composites,'' Composites, **29A**, pp. 619–626.

[10] Aboudi, J., 1989, ''Micromechanical Analysis of Composites by the Method of Cells,'' Appl. Mech. Rev., **42**, No. 7, pp. 193–221.

[11] Sun, C. T., and Vaidya, R. S., 1996, ''Prediction of Composite Properties From a Representative Volume Element,'' Compos. Sci. Technol., **56**, pp. 171–179.

[12] Hyer, M. W., 1998, *Stress Analysis of Fiber-Reinforced Composite Materials*, McGraw-Hill, New York.

[13] Adams, D. F., 1987, ''A Micromechanics Analysis of the Influence of the Interface on the Performance of Polymer-Matrix Composites,'' J. Reinforced Plastics Compos., **6**, pp. 66–88.

[14] Nassehi, V., Dhillon, J., and Mascia, L., 1993, ''Finite Element Simulation of the Micromechanics of Interlayered Polymer/Fibre Composites: A Study of the Interactions Between the Reinforcing Phases,'' Compos. Sci. Technol., **47**, pp. 349–358.

[15] Mukherjee, S., 1982, *Boundary Element Methods in Creep and Fracture*, Applied Science Publishers, New York.

[16] Cruse, T. A., 1988, *Boundary Element Analysis in Computational Fracture Mechanics*, Kluwer, Dordrecht, The Netherlands.

[17] Banerjee, P. K., 1994, *The Boundary Element Methods in Engineering*, McGraw-Hill, New York.

[18] Cruse, T. A., 1996, ''BIE Fracture Mechanics Analysis: 25 Years of Developments,'' Computational Mech., **18**, pp. 1–11.

[19] Oshima, N., and Watari, N., 1992, ''Calculation of Effective Elastic Moduli of Composite Materials With Dispersed Parallel Fibers,'' *Theoretical and Applied Mechanics*, M. Hori and G. Yagawa, eds., Japan National Committee for Theoretical and Applied Mechanics, Science Council of Japan, **41**, pp. 181–188.

[20] Gulrajani, S. N., and Mukherjee, S., 1993, ''Sensitivities and Optimal Design of Hexagonal Array Fiber Composites With Respect to Interphase Properties,'' Int. J. Solids Struct., **30**, No. 15, pp. 2009–2026.

[21] Pan, L., Adams, D. O., and Rizzo, F. J., 1998, ''Boundary Element Analysis for Composite Materials and a Library of Green's Functions,'' Comput. Struct., **66**, No. 5, pp. 685–693.

[22] Krishnasamy, G., Rizzo, F. J., and Liu, Y. J., 1994, ''Boundary Integral Equations for Thin Bodies,'' Int. J. Numer. Methods Eng., **37**, pp. 107–121.

[23] Gray, L. J., Martha, L. F., and Ingraffea, A. R., 1990, ''Hypersingular Integrals in Boundary Element Fracture Analysis,'' Int. J. Numer. Methods Eng., **29**, pp. 1135–1158.

[24] Krishnasamy, G., Rizzo, F. J., and Rudolphi, T. J., 1991, ''Hypersingular Boundary Integral Equations: Their Occurrence, Interpretation, Regularization, and Computation,'' *Developments in Boundary Element Methods*, Vol. VII, P. K. Banerjee et al., eds., Elsevier Applied Science Publishers, London, Chapter 7.

[25] Liu, Y. J., and Rizzo, F. J., 1997, ''Scattering of Elastic Waves From Thin Shapes in Three Dimensions Using the Composite Boundary Integral Equation Formulation,'' J. Acoust. Soc. Am., **102**, No. 2, Pt. 1, Aug., pp. 926–932.

[26] Liu, Y. J., 1998, ''Analysis of Shell-Like Structures by the Boundary Element Method Based on 3-D Elasticity: Formulation and Verification,'' Int. J. Numer. Methods Eng., **41**, pp. 541–558.

[27] Luo, J. F., Liu, Y. J., and Berger, E. J., 1998, ''Analysis of Two-Dimensional Thin Structures (From Micro-to Nano-scales) Using the Boundary Element Method,'' Computational Mech., **22**, pp. 404–412.

[28] Mukherjee, S., 1999, ''On Boundary Integral Equations for Cracked and for Thin Bodies,'' Math. Mech. Solids, in press.

[29] Cruse, T. A., and Aithal, R., 1993, ''Non-singular Boundary Integral Equation Implementation,'' Int. J. Numer. Methods Eng., **36**, pp. 237–254.

[30] Huang, Q., and Cruse, T. A., 1993, ''Some Notes on Singular Integral Techniques in Boundary Element Analysis,'' Int. J. Numer. Methods Eng., **36**, pp. 2643–2659.

[31] Liu, Y. J., Zhang, D., and Rizzo, F. J., 1993, ''Nearly Singular and Hypersingular Integrals in the Boundary Element Method,'' *Boundary Elements XV*, C. A. Brebbia and J. J. Rencis, eds., Computational Mechanics Publications, Southampton, UK, pp. 453–468.

[32] Rudolphi, T. J., 1991, ''The Use of Simple Solutions in the Regularization of Hypersingular Boundary Integral Equations,'' Mathl. Comput. Modelling, **15**, pp. 269–278.

[33] Liu, Y. J., and Rudolphi, T. J., 1991, ''Some Identities for Fundamental Solutions and Their Applications to Weakly-Singular Boundary Element Formulations,'' Eng. Anal. Boundary Elem., **8**, No. 6, pp. 301–311.

[34] Chandrupatla, T. R., and Belegundu, A. D., 1997, *Introduction to Finite Elements in Engineering*, 2nd Ed., Prentice-Hall, Englewood Cliffs, NJ.

[35] Timoshenko, S. P., and Goodier, J. N., 1987, *Theory of Elasticity*, 3rd Ed., McGraw-Hill, New York.